PCCP

Accepted Manuscript

ROYAL SOCIETY OF CHEMISTRY

www.rsc.org/pccp

Isn't the space charge potential in ceria-based solid electrolytes largely overestimated?

Sangtae Kim*

Department of Materials Science and Engineering, University of California, Davis, CA 95618, USA

*chmkim@ucdavis.edu

Abstract

The effective ionic conductivity of polycrystalline solid electrolytes that conduct oxide ions or protons is known to be markedly below that of the corresponding single crystals due to substantial current obstruction across the grain boundary. Numerous studies have previously demonstrated that the ionic charge carriers deplete in the vicinity of the grain boundary to form a potential barrier at the grain boundary, which further impedes the current across the grain boundary. Hence accurate estimation of the barrier height is essential to acquire a comprehensive and precise mechanistic picture of the ionic current in the solid electrolytes. The values of the potential barrier height, *i.e.* equivalent to the equilibrium space charge potential with the opposite sign, in prominent solid electrolytes such as ceria solid solutions are available in the literature and was determined exclusively from the ratio of the resistivity of the grain boundary to that of the crystal interior. Here I present the results clearly demonstrating that the resistivity ratio yields considerable overestimation of the barrier height even in relatively diluted solid solutions of ceria. These results implies that the space charge is unlikely the sole origin of the large current obstruction across the grain boundary in ceria-based solid electrolytes.

Introduction

It has been widely accepted that the ionic current across the grain boundaries in prominent ionic conductors currently being employed in conventional high-temperature solid oxide fuel cells (HT-SOFCs) or those being considered for next-generation intermediate-temperature SOFCs (IT-SOFCs) as solid electrolytes is obstructed largely due to the presence of space-charge zones adjacent to the grain-boundary core, where the ionic charge carriers are depleted.[1-14] The space-charge zone can be as wide as several Debye lengths, suppressing effective ionic conductivity of the solid electrolytes by orders of magnitude.[2, 15-17] Formation of such an extended depletion zone is attributed to a parabolic decay of the charge carrier concentration (in a logarithmic scale) in the vicinity of the grain-boundary core (namely a Mott-Schottky profile) as algebraically summarized below.

Let us consider a solid electrolyte with two majority point defects with opposite charges (*i.e.* an acceptor dopant and an ionic carrier). Due to substantial difference in the mobility between the two defects, the dopant cations are hardly mobile even at temperatures where HT-SOFCs are operated (~900°C). Consequently local variation in the dopant concentration, c_d, is minimal throughout the material (i.e. $\partial c_d(x)/\partial x = 0$ for a one dimensional problem), while the ionic charge carriers are depleted in the space-charge zone in order to compensate the excess charge trapped in the grain-boundary core (for the depletion, the mobile ions and the excess charge in the grain-boundary core repel each other). For large depletion, the charge density in the space-charge zone, $Q_{sc}(x) = \sum_j z_j q c_{j,sc}(x)$, is primarily fixed by c_d (the Mott-Schottky assumption), and the Poisson's equation can be simplified to,

$$\frac{\partial^2}{\partial x^2}\varphi(x) = -\frac{Q_{sc}(x)}{\varepsilon} \approx -\frac{z_d q c_{d,sc}}{\varepsilon}, \qquad (1)$$

where $\varphi(x)$ is local electrostatic potential, ε is a dielectric constant and z_d is the effective charge of the dopant which is typically -1 for most of the solid electrolytes of interest.

Integrating Eq. (1) with the boundary conditions, $\varphi'(\delta_{sc}) = 0$ and $\varphi(\delta_{sc}) = \varphi(\infty)$, results in[2, 8, 15]

$$\varphi_x = -\frac{z_d q c_{d,sc}}{\varepsilon}(x - \delta_{sc})^2 \qquad (2)$$

where the width of the space charge zone, δ_{sc}, is given as

$$\delta_{sc} = 2\left(L_D\sqrt{\varphi_0 / V_{th}}\right) \qquad (3)$$

with $z_d = -1$. Here $V_{th} = k_B T / q$ is the thermal voltage with k_B, q, and T being Boltzmann constant, elementary charge and absolute temperature. L_D is the Debye length. $\varphi_o = \varphi(0) - \varphi(\infty)$ is namely the potential barrier height, where $\varphi(0)$ and $\varphi(\infty)$ denote φ in the grain boundary core and φ sufficiently far from it, respectively. φ_0 is the prime parameter that can effectively characterize the degree of the depletion and thus the influence of the space-charge effect on ionic transport. (Recall that φ_0 is equivalent to the equilibrium space-charge potential with the opposite sign.) Hence accurate estimation of φ_0 is an essential step to characterize and even optimize the ionic current in the solid electrolytes.

The local concentration of the charge carrier, $c_i(x)$, can be given as a function of $\varphi_x = \varphi(x) - \varphi(\infty)$,

$$c_i(x) = c_i(\infty) \exp(-z_i \varphi_x / V_{th}) \tag{4}$$

at an electrochemical equilibrium (*i.e.* $\partial \tilde{\mu}_j(x) / \partial x = 0$ where the electrochemical potential is given as $\tilde{\mu}_j = \mu_j + z_j q \varphi$ with μ being the chemical potential for any mobile charge carrier *j*), the profile of which can be obtained by combining Eqs. (2) and (4),[2, 8, 15]

$$c_i(x) = c_i(\infty) \exp\left\{ -\left| \frac{z_i}{z_d} \right| \left(\frac{x - \delta_{sc}}{2L_D} \right)^2 \right\} \tag{5}$$

The corresponding local resistivity $\rho_i(x)$ relative to the bulk counterpart $\rho_{i\infty}$ then reads

$$\frac{\rho_i(x)}{\rho_{i\infty}} = \exp\left(\frac{2\varphi_x}{V_{th}} \right) \tag{6}$$

as $\rho(x) \propto c(x)^{-1}$.

According to the brick-layer model (BLM) [18], a grain boundary core is sandwiched between two space charge zones (namely back-to-back space-charge zones). The effective resistivity of a grain boundary ρ_{gb} can then be approximated as the resistivity across the space-charge zone ρ_{sc} ($\rho_{gb} \approx \rho_{sc}$):

$$\rho_{i,sc} = \frac{1}{2\delta_{sc}} \int_0^{2\delta_{sc}} \rho_i(x) dx \tag{7}$$

Combining Eqs. (6) and (7) yields[8, 18],

$$\frac{\rho_{i,sc}}{\rho_{i\infty}} = \frac{\exp(z_i\varphi_0 / V_{th})}{2z_i\varphi_0 / V_{th}} = \frac{\rho_{i,gb}}{\rho_{i\infty}} = r_{gb} \quad (8)$$

It is this resistivity ratio that has been exclusively used to determine φ_0 in the solid electrolytes with blocking serial grain boundaries to date. Since both $\rho_{i,gb}$ and $\rho_{i\infty}$ can be determined from a single impedance spectrum measured at a given temperature, φ_0 is readily available from Eq. (8). However it is important to realize that Eq. (8) is derived under the assumptions that: (i) the space charge is the sole source for current obstruction across the grain boundaries (i.e. $\rho_{i,sc} = \rho_{i,gb}$ in Eq, (8)) and (ii) the trapped charge is concentrated in a narrow region of the grain-boundary core and the space-charge zone is sufficiently wider than the core (*i.e.* the width of the back-to-back space-charge zones $\approx 2\delta_{sc}$, see Eq. (7)). These assumptions place an important limitation of applicability of Eq. (8) that φ_0 can be accurately determined by Eq. (8) only if these two assumptions are strictly fulfilled.

It is worth noting that the derivatives of the resistivity in Eq. (8) with respect to temperature result in,

$$E_{a,gb} - E_{a\infty} = (z_i q\varphi_0 - k_B T)\left\{1 + \frac{1}{T\varphi_0}\frac{d\varphi_0}{d\left(\frac{1}{T}\right)}\right\} \quad (10)$$

since the activation energy is given as $E_a \equiv \frac{d\ln\rho}{d\left(\frac{1}{k_B T}\right)}$. $E_{a,gb}$ and $E_{a\infty}$ denote the E_a of grain boundary and grain interior (hereafter bulk) resistivity, respectively.

Eq. (10) can be approximated to;

$$E_{a,gb} - E_{a\infty} \approx z_i q\left\{\varphi_0 + \frac{1}{T}\frac{d\varphi_0}{d\left(\frac{1}{T}\right)}\right\} \quad (11)$$

for large depletion ($\varphi_0 >> V_{th}$).

The last term on the right hand side of Eq. (11) concerns the temperature dependence of φ_0, which is often insignificant compared to φ_0 especially within a relatively narrow range of temperature. Eq. (11) can then be further simplified to

$$E_{a,gb} - E_{a\infty} \approx z_i q\varphi_0 \quad (12)$$

Eq. (12) indicates straightforwardly that φ_0 serves as an extra barrier for ion migration across the grain boundary and can be rearranged to

$$\varphi_0 \approx \frac{E_{a,gb} - E_{a\infty}}{z_i q} \quad (13)$$

Consequently, alternative to Eq. (8), φ_0 can then be estimated by Eq. (13) as well by simply taking the difference between $E_{a,gb}$ and $E_{a\infty}$ in the solid electrolytes experimentally measured and the effective charge of the carriers. Although Eq. (13) allows for only a rough estimate of φ_0 due to the uncertainty in the temperature dependence of φ_0, the value of φ_0 calculated from Eqs. (8) and (13) should still be reasonably consistent with one another at a given temperature as long as $\varphi_0 >> V_{th}$ (namely "the consistency check"). In fact this consistency check is a must to confirm the φ_0 determined using Eq. (8) since $E_{a,gb}$ directly indicates φ_0 on top of $E_{a\infty}$ as previously mentioned (Eq. (12)) while Eq. (8) takes the absolute value of the grain-boundary resistance R_{gb} experimentally measured, which may not always be consistent with the resistance across the back-to-back space-charge zones, R_{sc}. For instance, if the current across the grain boundary was further constricted due to the presence of e.g. an insulating secondary phase, R_{gb} would be greater than R_{sc}. Whereas such current constriction will have little effects on $E_{a,gb}$, it will increase r_{gb} in Eq. (8), resulting in overestimation of φ_0 when Eq. (8) is used. However in the vast majority of studies previously reported, φ_0 in various solid electrolytes was estimated using Eq. (8) only and the consistency check has been neglected.

In this contribution, I present the results that the value of φ_0 in Gd-doped CeO_2 (GDCx with x being 1, 3, 5, 10, 15, 20 cat. % Gd) determined from Eq. (8) is noticeably higher than that estimated by Eq. (13). As will be demonstrated below, this is true even for lightly doped ceria in which the space charge was reported to be a prime cause of the grain-boundary resistance. Furthermore the discrepancy becomes larger as the Gd content in the material increases. Such a failure of the consistency check strongly suggests that the current obstruction across the grain boundary in ceria-based solid electrolytes is attributed to multiple origins (i.e. $R_{gb} > R_{sc}$) and the space charge plays only a minor role in practically important heavily doped ceria.

Results and Discussion

The Arrhenius plots of the effective resistivities in the bulk and across a single grain boundary in GDCx are presented in Figure 1 as a function of c_d. The former was computed using the relation $\rho_\infty = R_\infty (l/A)$ with *R* being the resistance, *A* and *l* the electrode area and the distance between two electrodes, respectively.

The latter is calculated using the equation $\rho_{gb} = (\tau_{gb} / \tau_{\infty})\rho_{\infty}$ derived under the assumptions that the local variation in ε throughout the material is negligibly small. For the derivation the BLM is also applied. τ denotes relaxation time given by the product of *R* and capacitance *C*. The *R* and *C* in the bulk and at the grain boundary in GDCx were determined at various temperatures using ac-impedance spectroscopy. Interpretation of impedance spectra measured from a polycrystalline ceramic to determine those parameters using an appropriate equivalent circuit has been well established and won't be discussed further here for GDCx.

Two aspects are evident from Figure 1: i) The ρ_{gb} is much larger than the corresponding ρ_{∞} regardless of c_d and the difference sharply increases as c_d decreases to become as large as ~8 orders of magnitude in the temperature range of interest. ii) The $E_{a,gb}$ is substantially higher than the bulk counterpart for the lightly doped samples and rapidly approaches the bulk value as c_d increases. Such a drastic change in $E_{a,gb}$ with c_d can be seen more clearly in Figure 2. In contrary, the $E_{a\infty}$ remains nearly constant up to GDC5 and slowly increases as c_d further increases. It has been widely accepted that the increase in $E_{a,\infty}$ with c_d in doped ceria is attributed to the increase in the electrostatic interactions between the oxygen vacancies and the dopant cations. Further discussion on this subject is beyond the scope of the present study and can be found elsewhere[19].

Let us assume that the relatively large ρ_{gb} in GDCx is exclusively due to the space charge (i.e. $R_{gb} = R_{sc}$) to make use of Eq. (8) in determining φ_0 as done in the vast majority of the studies previously reported. The values of φ_0 at 325°C calculated using Eq, (8) are listed in Table 1 and are also plotted in Figure 3 as a function of c_d. The actual c_d is found to be slightly higher than nominal c_d for the lightly doped (x < 10) samples. We note that φ_0 determined even for the most heavily doped sample (GDC20) is still considerably high (0.27 V) due to large r_{gb} > ~1000 (Figure 1).

Now we discuss the result of the consistency check carried out using Eq. (13) to confirm the values of φ_0 listed in Table 1, which can also be found in Table 1. As Figure 2 clearly shows, the difference between $E_{a,gb}$ and $E_{a\infty}$ for GDCx with x > 10 quickly approaches to zero, indicating that φ_0 rapidly reduces with c_d to become insignificant in the heavily doped samples (Eq. 12) as illustrated in Figure 3. The values of φ_0 resulted from Eq. (8) are higher than those determined by Eq, (13) regardless of c_d and the discrepancy

is already substantial (> 0.2 eV) for GDC3. Such noticeable disagreement between φ_0 estimated by Eqs. (8) and (13) is far beyond the uncertainty associated with the temperature dependence of φ_0. It is thus evident that the consistency check fails for GDCx where x ≥ 2 and that Eq. (8) overestimates φ_0 even for GDC with such relatively low c_d. Furthermore the grain boundaries in practically important GDCx with 10 ≤ x ≤ 20 are still highly blocking although φ_0 in those materials approaches zero ($E_{a,gb} \approx E_{a\infty}$). This result strongly suggests that besides the space charge there must be extra causes that obstruct the current across the grain boundaries in GDCx. Detailed information about the origins of such extra causes contributing to R_{gb} (i.e. $R_{gb} = R_{sc} + R_{ex}$) in GDCx is currently lacking and beyond the scope of the present study.

A new approach that allows for more accurate estimation of φ_0 by interpreting the current – voltage characteristics of grain boundaries in ceria has recently been reported by Kim et al.[20-22] The φ_0 estimated for GDC3 by this new method at 325°C is ~ 0.3 V. They have also demonstrated that φ_0 remains nearly constant in a sufficiently narrow range of temperature. This value is slightly higher than that (0.23 V) determined by Eq. (13). Nonetheless the discrepancy is rather small considering the fact that Eq. (13) provides only a rough estimate and that the actual dopant concentration in GDC3 in the present study is ~3.6 cat.%. On the other hand, the φ_0 is still considerably lower than the value (0.45 V) calculated using Eq. (8), supporting that Eq. (13) overestimates φ_0.

Conclusion

The importance of the consistency between φ_0 resulted from Eqs, (8) and Eq. (13) to warrant the accuracy of the φ_0 has been demonstrated. Since Eq. (8) assumes that current obstruction across a grain boundary is exclusively due to the space charge, it will overestimate φ_0 if the grain boundary resistance has extra causes other than the space charge. However, most of the φ_0 values available in the literature were determined only from Eq, (8) and the possibility of such overestimation has been overlooked. The systematic investigations on φ_0 in GDCx with x = 1, 3, 5, 10, 15, 20 cat.% using both Eqs. (8) and (13) clearly demonstrate that the value of φ_0 determined by Eq. (8) is substantially higher than the corresponding value from Eq. (13) when x ≥ ~2. It is important to note that the current across the grain boundary in GDCx with x > 10 is still severely obstructed although φ_0 in those concentrated solid solutions seems to be

insignificant ($E_{a,gb} \approx E_{a\infty}$). These results unambiguously demonstrate that besides the space charge, extra causes for the large R_{gb} are present even in lightly doped GDC, which becomes dominant in the heavily doped solid electrolytes.

Experimental

The GDCx powders were synthesized via a co-precipitation method using $Gd(NO_3)_3 \cdot 6H_2O$ (Aldrich, 99.9% purity) and $Ce(NO_3)_3 \cdot 6H_2O$ (Strem Chemicals, 99.9% purity). The precipitates were collected by centrifugation and washed with distilled water and alcohol several times. The obtained powders were dried at 120 °C for 12 h, followed by annealing at 700 °C under air for 2 h. (See Ref.[5] for more in detail.) The resulting power was pressed into cylindrical pellets using a cold isostatic press at 276 MPa and the pellets were sintered at 1400 °C for 5 h under air, with heating and cooling rates of 5° C/min. The relative density of all the sintered pellets was determined by an Archimedes method and greater than 95%.

The impedance measurements of the dense GDCx pellets with Pt electrodes were carried out under air in the temperature range of 100 - 700 °C, using a Novocontrol Alpha – AN modulus analyzer in the frequency range of 10^{-1} – 10^{7} Hz. The fittings of the obtained impedance spectra (i.e. Nyquist plots) with an appropriate equivalent circuit model were done using the software Z-View.

Acknowledgement

S. K. thanks the US–Israel Binational Science Foundation (2012237) for funding this research.

References

1. S. Kim and J. Maier, *J Electrochem Soc*, 2002, 149, J73-J83.
2. S. Kim, J. Fleig and J. Maier, *Phys Chem Chem Phys*, 2003, 5, 2268-2273.
3. H. J. Park and S. Kim, *J Phys Chem C*, 2007, 111, 14903-14910.
4. H. J. Park and S. Kim, *Solid State Ionics*, 2008, 179, 1329-1332.
5. H. J. Avila-Paredes, K. Choi, C. T. Chen and S. Kim, *J Mater Chem*, 2009, 19, 4837-4842.
6. C. T. Chen, C. E. Daniel and S. Kim, *J Mater Chem*, 2011, 21, 5435-5442.
7. F. Iguchi, C. T. Chen, H. Yugami and S. Kim, *J Mater Chem*, 2011, 21, 16517-16523.
8. X. Guo and R. Waser, *Prog Mater Sci*, 2006, 51, 151-210.
9. M. C. Gobel, G. Gregori and J. Maier, *Phys Chem Chem Phys*, 2014, 16, 10214-10231.
10. A. Tschope, S. Kilassonia and R. Birringer, *Solid State Ionics*, 2004, 173, 57-61.
11. F. Iguchi, N. Sata, T. Tsurui and H. Yugami, *Solid State Ionics*, 2007, 178, 691-695.
12. C. Kjolseth, H. Fjeld, O. Prytz, P. I. Dahl, C. Estournes, R. Haugsrud and T. Norby, *Solid State Ionics*, 2010, 181, 268-275.
13. B. J. Nyman, E. E. Helgee and G. Wahnstrom, *Appl Phys Lett*, 2012, 100.
14. M. Shirpour, R. Merkle, C. T. Lin and J. Maier, *Phys Chem Chem Phys*, 2012, 14, 730-740.
15. J. Maier, *Prog Solid State Ch*, 1995, 23, 171-263.
16. A. Tschope, *Solid State Ionics*, 2001, 139, 267-280.
17. R. A. De Souza, *Phys Chem Chem Phys*, 2009, 11, 9939-9969.
18. S. Rodewald, J. Fleig and J. Maier, *J Am Ceram Soc*, 2001, 84, 521-530.
19. S. Buyukkilic, S. Kim and A. Navrotsky, *Angew Chem Int Edit*, 2014, 53, 9517-9521.
20. S. Kim, S. K. Kim, S. Khodorov, J. Maier and I. Lubomirsky, *Phys Chem Chem Phys*, 2016, 18, 3023-3031.
21. S. K. Kim, S. Khodorov, C. T. Chen, S. Kim and I. Lubomirsky, *Phys Chem Chem Phys*, 2013, 15, 8716-8721.
22. S. K. Kim, S. Khodorov, I. Lubomirsky and S. Kim, *Phys Chem Chem Phys*, 2014, 16, 14961-14968.

Table 1. The dopant concentration, activation energies, and potential barrier heights determined for GDCx.

Nominal c_d [cat. %]	Actual c_d [cat. %]	$E_{a,gb}$ [eV]	$E_{a\infty}$ [eV]	$(E_{a,gb}- E_{a\infty})/2q$ [V]	φ_0 from Eq. (8) at 325°C [V]
1	1.8 ± 0.5	1.61	0.71	0.45	0.54
3	3.6 ± 0.7	1.14	0.69	0.23	0.45
5	5.8 ± 0.6	1.00	0.70	0.15	0.36
10	10.9 ± 0.5	0.90	0.74	0.08	0.34
15	15.7 ± 0.6	0.93	0.85	0.04	0.29
20	19.8 ± 0.9	1.01	0.97	0.02	0.27

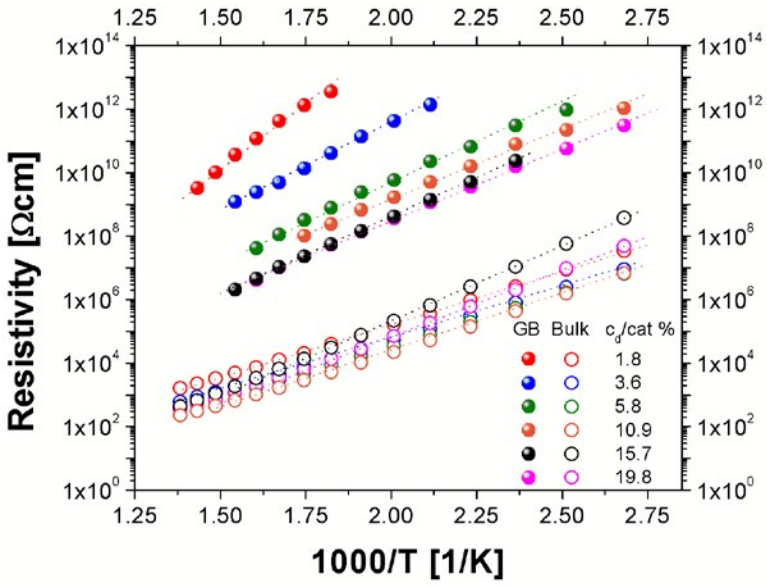

Figure 1. The Arrhenius plots of the resistivity of both bulk and grain boundary in GDCx. The dotted line is only a guide to the eye.

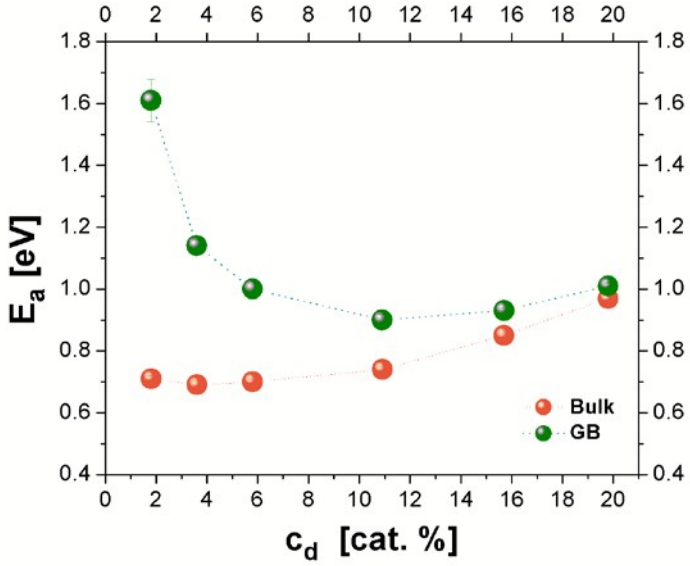

Figure 2. The activation energy of both the bulk and grain boundary resistivity in GDC as a function of the dopant concentration (replotted using the data from Ref.[5]). The dotted line is only a guide to the eye.

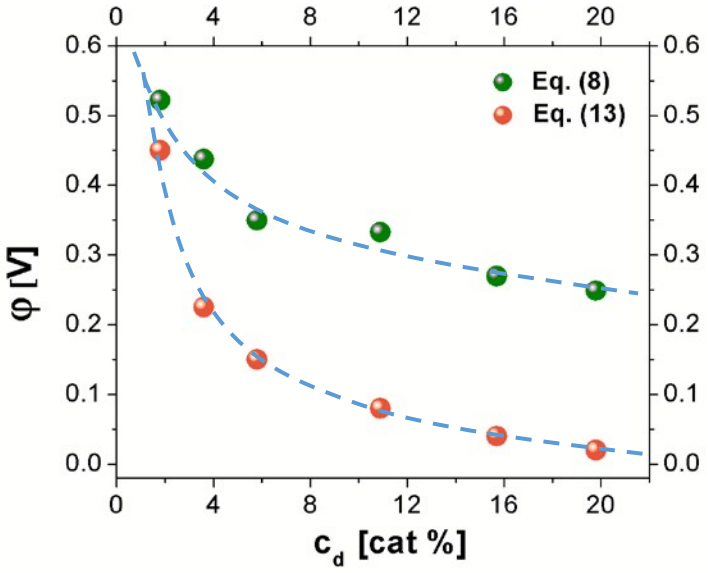

Figure 3. The potential barrier height in GDC determined from Eqs. (8) and (13) as a function of the dopant concentraion. The dotted line is only a guide to the eye.

TOC Graphic

The height of the potential barrier at the grain boundary in concentrated ceria solid solutions found in the literature is largely overestimated.